Biotechnology Journal

DOI 10.1002/biot.201000340

Biotechnol. J. 2011, 6, 204–212

Research Article

A three-dimensional in vitro ovarian cancer coculture model using a high-throughput cell patterning platform

*Feng Xu[1]**, Jonathan Celli[2]**, Imran Rizvi[2], Sangjun Moon[1], Tayyaba Hasan[2,3]* and Utkan Demirci[1,3]*

[1] Demirci Bio-Acoustic-MEMS in Medicine (BAMM) Laboratory, Center for Biomedical Engineering, Department of Medicine, Brigham and Women's Hospital and Harvard Medical School, Boston, MA, USA
[2] Wellman Center for Photomedicine, Massachusetts General Hospital, Harvard Medical School, Boston, MA, USA
[3] Harvard-MIT Health Sciences and Technology, Cambridge, MA, USA

In vitro 3D cancer models that provide a more accurate representation of disease in vivo are urgently needed to improve our understanding of cancer pathology and to develop better cancer therapies. However, development of 3D models that are based on manual ejection of cells from micropipettes suffer from inherent limitations such as poor control over cell density, limited repeatability, low throughput, and, in the case of coculture models, lack of reproducible control over spatial distance between cell types (e.g., cancer and stromal cells). In this study, we build on a recently introduced 3D model in which human ovarian cancer (OVCAR-5) cells overlaid on Matrigel™ spontaneously form multicellular acini. We introduce a high-throughput automated cell printing system to bioprint a 3D coculture model using cancer cells and normal fibroblasts micropatterned on Matrigel™. Two cell types were patterned within a spatially controlled microenvironment (e.g., cell density, cell-cell distance) in a high-throughput and reproducible manner; both cell types remained viable during printing and continued to proliferate following patterning. This approach enables the miniaturization of an established macro-scale 3D culture model and would allow systematic investigation into the multiple unknown regulatory feedback mechanisms between tumor and stromal cells and provide a tool for high-throughput drug screening.

Received 11 October 2010
Revised 14 December 2010
Accepted 15 December 2010

Supporting information available online

Keywords: Cell patterning · 3D ovarian coculture cancer model · Drug screening · High throughput

1 Introduction

The majority of ovarian cancer patients are diagnosed after the disease has metastasized to local and distant sites [1]. The survival rate remains low (approx. 30%) mostly due to residual disease, which does not fully respond to the consecutive chemotherapy treatment [2]. It is clear that new treatments are urgently needed to improve the clinical management of this deadly disease. Inadequate progress in this area is partly due to poor predictive capability of traditional cell culture models for evaluation of therapeutic efficacy. This situation points to the need for in vitro cancer models that more accurately emulate human disease in vivo for high-throughput assessment of new therapies. A variety of models for in vitro cancer growth and treatment have made significant advances toward mimicking in vivo tumor architecture and growth behavior as compared to cells grown on flat 2D tissue culture substrates.

In vivo, tumors are complex tissues composed of, in the case of carcinomas, stromal cells such as fibroblasts [3, 4] and endothelial cells [5, 6]. Fibroblasts are among the most important stromal signaling partners found within the various forms

Correspondence: Dr. Utkan Demirci, Harvard-MIT Health Sciences and Technology, Cambridge, MA, USA
E-mail: udemirci@rics.bwh.harvard.edu

* Additional corresponding author: Dr. Tayyaba Hasan
E-mail: thasan@partners.org
** These authors contributed equally to this work.

of human carcinomas [7]. Fibroblasts are associated with cancer cells at all stages of cancer progression, and have been linked to different tumor growth and metastasis activities. For example, fibroblasts could play an important role in promoting ovarian cancer growth and progression [8]. Fibroblasts are thus a key determinant in the malignant progression of cancer and represent an important target for cancer therapies [9]. Therefore, platforms to study the effect of stromal cells on cancer are urgently needed.

It has been traditionally difficult to pattern cocultures of cells. The manual methods do not provide control over cell position within a biologically relevant scale, which ranges from tens to hundreds of micrometers. The newer approaches to create such microcontrol over patterning of multiple cell types include stencils [10] and microelectromechanical system (MEMS) [11] approaches. Approaches based on stencils are limited by fabrication challenges [12]. In addition, it is difficult to control the adherence and response of different cell types based on stencil material properties. Some of the MEMS approaches use clickwise manual attachment of gears on the stencils to control cell-to-cell distance [11]. However, this platform requires microfabrication techniques such as deep reactive ion etching (DRIE) or chemical etching on silicon, which are expensive and suffer from low cell adhesion and imaging problems since silicon is not transparent. Such techniques are also low throughput since pieces have to be manually assembled. Here, we introduce a simple method that only involves the patterning of multiple cell types to predetermined locations.

In the present study, we utilized an innovative cell printing approach that overcomes inherent limitations of manually ejecting cells via a pipette, which enabled us to pattern ovarian cancer cells and normal fibroblasts at fixed spatial separations on a Matrigel substrate. In the 3D patterned overlay coculture model developed here, based on a previously described manually pipetted model, cells spontaneously form 3D acinar structures after adhering to the Matrigel surface [13, 14].

Currently, cancer biology experiments mostly use pipette-patterned large gel structures, where a few thousands of cells are plated in tens of microliters of gels with a low patterning precision capability of a few millimeters. The low control precision in placement of these distinct cell types has restricted their use in systematic investigations of such crucial tumor-stroma interactions where resolution of tens of microns in the placement of distinct populations is needed. To address these challenges with manual pipette ejection of cells, possible technologies include cell printing [15–21], negative dielectrophoresis [22] and microfluidic patterning technologies [23, 24].

The focus of this paper is the creation of well-patterned biological acini structures using a printing method. This work addresses unique challenges in the sense that the cells have to be both viable and form 3D functional acini units. As an in vitro model of ovarian cancer, we demonstrate a cell patterning platform that prints two types of cells onto Matrigel, where the acini formed using this platform post-pattering recapitulate the morphology and growth kinetics previously reported for cells deposited by manual pipetting. We present the technique and its biological proof of concept; it represents an elegant approach for miniaturization of an established macro-scale 3D culture model. The novelty of this work comes from: (1) the combination of state-of-the-art cell biopatterning with cancer biology to build in vitro 3D ovarian cancer models at high throughput that are capable of recreating distinct in vitro cancer models under well-defined and reproducible conditions; and (2) the potential of the technology as a tool for delving into coculture interaction between cancer and stromal cells that may be otherwise overshadowed by manual handling and culturing methods.

2 Materials and methods

2.1 Cell preparation

NIH: OVCAR-5 cells (an epithelial human ovarian cancer cell line) were obtained from Thomas Hamilton (Fox Chase Cancer Institute, Philadelphia, PA). MRC-5 cells (normal human fibroblast cell line) were obtained from ATCC. Both cells lines were cultured in a CO_2 water-jacketed incubator at 37°C, 5% CO_2 (Forma Scientific, Model 3110) and passaged under sterile conditions. The cell media were prepared by mixing 500 mL 1× RPMI (RPMI 1640 with L-glutamine, Cellgro, 10-040-CV) for OVCAR-5 or 1× MEM (MEM with Earle's Salts and L-glutamine, Cellgro, 10-010-CV) for MRC-5 with 50 mL fetal bovine serum (FBS, Gibco, 10439-024) and 5 mL 1% penicillin-streptomycin (pen/strep, Sigma, P4333) through a sterile filter (500 mL Express Plus 0.22-μm membrane, Millipore, 5179-SCGPU05RE). After confluence, the cells were collected through trypsinization and centrifugation. Initial cell concentration of cell suspensions was calculated using 0.4% Trypan blue solution (for use with the Countess" automated cell counter, Invitrogen, T10282) and a hemacytometer (Hausser Scientific, 1483). The required cell concentrations

(1×10^6, 2×10^6, 5×10^6 and 10×10^6 cells/mL) were prepared by diluting with the cell medium.

2.2 Matrigel substrate preparation

A bed of growth factor-reduced (GFR) Matrigel™ (BD, 354230) was prepared prior to cell printing on each culture dish (35 mm in diameter, MatTek Corporation, P35G-1.0-20-C). GFR Matrigel™ was thawed overnight at 4°C on ice and was kept cool on ice before use. GFR Matrigel™ (150 μL) was added to the central glass bottom portion of each dish to produce a ~250-μm-thick basement membrane for overlay cell printing. All pipettes, tips, and tubes were pre-cooled on ice to prevent premature gelation of Matrigel™.

2.3 Cell-encapsulating droplet patterning

We have already developed and described a cell biopatterning system [25, 26]. Briefly, the system consists of an automated micrometer-resolution xyz stage (Precision Linear Stage, Newmark systems, NLS4) controlled by a stage controller (Newmark Systems, DMC-21x3) and nanoliter dispensing valves (Solenoid valve ejector, TechElan, G100-150300NJ) controlled by a pulse generator (Hewlett Packard, 8112A) (Fig. 1). The entire setup is enclosed within a sterile hood allowing long-term cultures of up to 3 weeks for patterned ovarian cancer model constructs. Here, two ejectors were used, one for ejecting OVCAR-5 and the other for ejecting MRC-5. The ejectors were connected to pressured nitrogen gas through a syringe reservoir. We used a valve ejector with a wide nozzle (with nozzle diameter 150 μm) to minimize local shear force created within the droplet during generation. This offers high post-ejecting cell viability. The stage and dispensing subsystems were synchronized and programmed. The cell suspensions of OVCAR-5 and MRC-5 were pipetted into two 10-mL syringe reservoirs, respectively. The valve opening duration and gas pressure were regulated to control the droplet size. Individual cell-encapsulating droplets were patterned at pre-determined positions on the GFR Matrigel™-coated glass-bottom culture dish. The dishes with patterned cells were then cultured with 2% GFR Matrigel™ media. Before and after cell patterning, the ejector was washed out with 70% ethanol and deionized water to sterilize the ejector.

2.4 Characterization of cell-encapsulating droplet

The size of each droplet was determined by ejecting droplets into a petri dish (60 × 15 mm) filled with liquid nitrogen. The frozen droplets were imaged using a microscope (Eclipse TE-2000 U, Nikon). Droplet diameters were obtained by fitting circles around each droplet image using ImageJ (NIH, Bethesda, MD). To assess the number of cells in individual ejected droplets, we used constant valve opening duration (60 μs) and gas (nitrogen) pressure (34.5 kPa) for constant droplet size. The valve opening time and the gas pressure determine the size of the generated droplets and how fast the droplets are ejected [25–27]. We then stained the ejected cells with DAPI (dilactate, Sigma-Aldrich, D9564) for counting the number of cells in individual droplets. Both bright-field and florescent images of the ejected cell-encapsulating droplets were viewed under the microscope (Nikon TE2000) immediately after printing. The numbers of cells were counted using ImageJ.

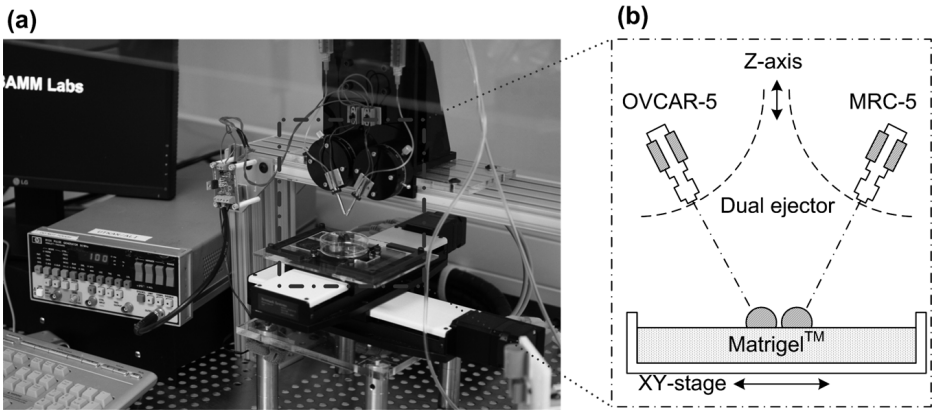

Figure 1. Schematic of a high-throughput ejector platform composed of a computerized stage and two ejectors. Dual ejector heads are used to eject different cell types simultaneously, i.e., cancer cells (OVCAR-5) and fibroblasts (MRC-5). (a) The platform is installed in a sterile hood to prevent contamination using HEPA filters. (b) The platform consists of an automated xyz stage and nanoliter dispensing valves controlled by a pulse generator. The position of substrate and droplet generator are synchronized and programmed through predefined control commands.

2.5 Cell viability test

Cell viability was assessed using a live/dead viability staining kit (Live/Dead Viability/Cytotoxicity Kit for mammalian cells, Invitrogen, L3224). Pre-ejection cell viability was measured in samples taken directly from the cell solutions as a control. Post-ejection cell viability was measured from ejected droplets at both 4 h and 3 days post printing to investigate the effects of cell ejection process and different cell patterns. Basically, the dishes containing the patterned cells were washed with PBS, stained for 10 min at 37°C with live/dead staining solution and then washed with PBS again prior to imaging under a fluorescent microscope (Nikon Eclipse TE-2000 U).

2.6 Characterization of acini growth

The patterned cells were monitored for 15 days using an inverted microscope (Zeiss Axiovert at the Wellman Center for Photomedicine) to acquire longitudinal dark-field microscopy images. Image data were processed at high throughput using custom MATLAB scripts (Mathworks, Natick, MA, USA) as reported earlier [14]. Basically, the images were first thresholded, made binary and then segmented to identify individual acini, which were then used to calculate size distributions and size change with time in temporally sequenced directories of dark-field image data.

2.7 Imaging 3D acinar structure using two-photon microscopy

To confirm the 3D acinar structure formed by patterned cancer cells, two-photon imaging (Olympus FV1000 MPE at the Wellman Center for Photomedicine) of endogenous fluorescent species using 750 nm excitation as previously described [28] was used to image printed 3D acini.

3 Results and discussions

3.1 Characterization of OVCAR-5 and MRC-5 patterning

We first characterized the spatial patterning precision through investigating individual droplet placement and inter-droplet distance. The droplet deposition variation was 4.9 μm and 18 μm in the distal and proximal directions, respectively, as reported in our earlier study [26]. The difference between programmed distance ($D_{program}$) and actual printed distance of droplets after patterning (D_{actual}) was <3.5% (Fig. 2a). The droplet ejection directionality determined this patterning variation. To measure the droplet size, droplets were ejected into liquid nitrogen (LN_2) using the method previously described [27] (see Supporting information, Fig. S1). The droplet diameter in LN_2 was measured under a microscope and the average size was 510 ± 26 μm (mean ± SD, n=51) as shown in Fig. 2b. When the droplets were ejected onto a substrate (i.e., Matrigel™), they spread out after landing (Fig. S1a).

Control over the number of cells in droplets can be achieved by changing the droplet size or the initial loading cell concentration. In this study, we used constant droplet size and only adjusted the cell concentration in the cell/medium mixture. Four different cell concentrations were used (1×10^6, 2×10^6, 5×10^6 and 10×10^6 cells/mL). The relationships between the number of cells per droplet and the cell concentration for OVCAR-5 and MRC-5 are shown in Fig. 2c, which clearly shows that the number of cells per droplet increases with increasing cell loading concentration. OVCAR-5 and MRC-5 were stained and compared under bright-field and UV light (see Supplementary Fig. S2). Mean ± SD at each concentration were 9 ± 1, 23 ± 3, 52 ± 2, 92 ± 5 cells/droplet (n=10) at 1×10^6, 2×10^6, 5×10^6 and 10×10^6 cells/mL for OVCAR-5, and 9 ± 1, 19 ± 2, 48 ± 7.3, 115 ± 10 cells/droplet (n=10) at 1×10^6, 2×10^6, 5×10^6 and 10×10^6 cells/mL for MRC-5. We chose a concentration of 52 ± 2 cells/droplet for acini growth experiments in culture. This cell concentration gave an average cell-to-cell distance of ~50 μm within the droplet and there is small variation (± 4%) of the number of encapsulated cells between two different cell types. These results prove that we can effectively control the initial cell density in the created constructs. Each cell-encapsulating droplet has on average the same number of cells. This is important because the number of cells per droplet determines the average cell-to-cell distance. Cell viability was assessed for three different cases, i.e., OVCAR-5 only, MRC-5 only, and cocultures of OVCAR5 and MRC-5 (Figs. 2d–f). The average cell viability relative to the culture control were 100%, 96.2%, 100%, 100% for only OVCAR-5, MRC-5 only, OVCAR5 in coculture and MRC-5 in coculture at 4 h post patterning, indicating that the ejection process did not have a detrimental effect on the cell viability. At 72 h post patterning, the coculture of patterned cancer cells and fibroblasts did not show any dead cells, whereas the OVCAR5 and MRC-5 viabilities were 93.8% and 90.1%, respectively.

It takes less than 100 μs (60 μs valve opening) to generate one droplet. With our current platform (two ejectors), we were able to generate

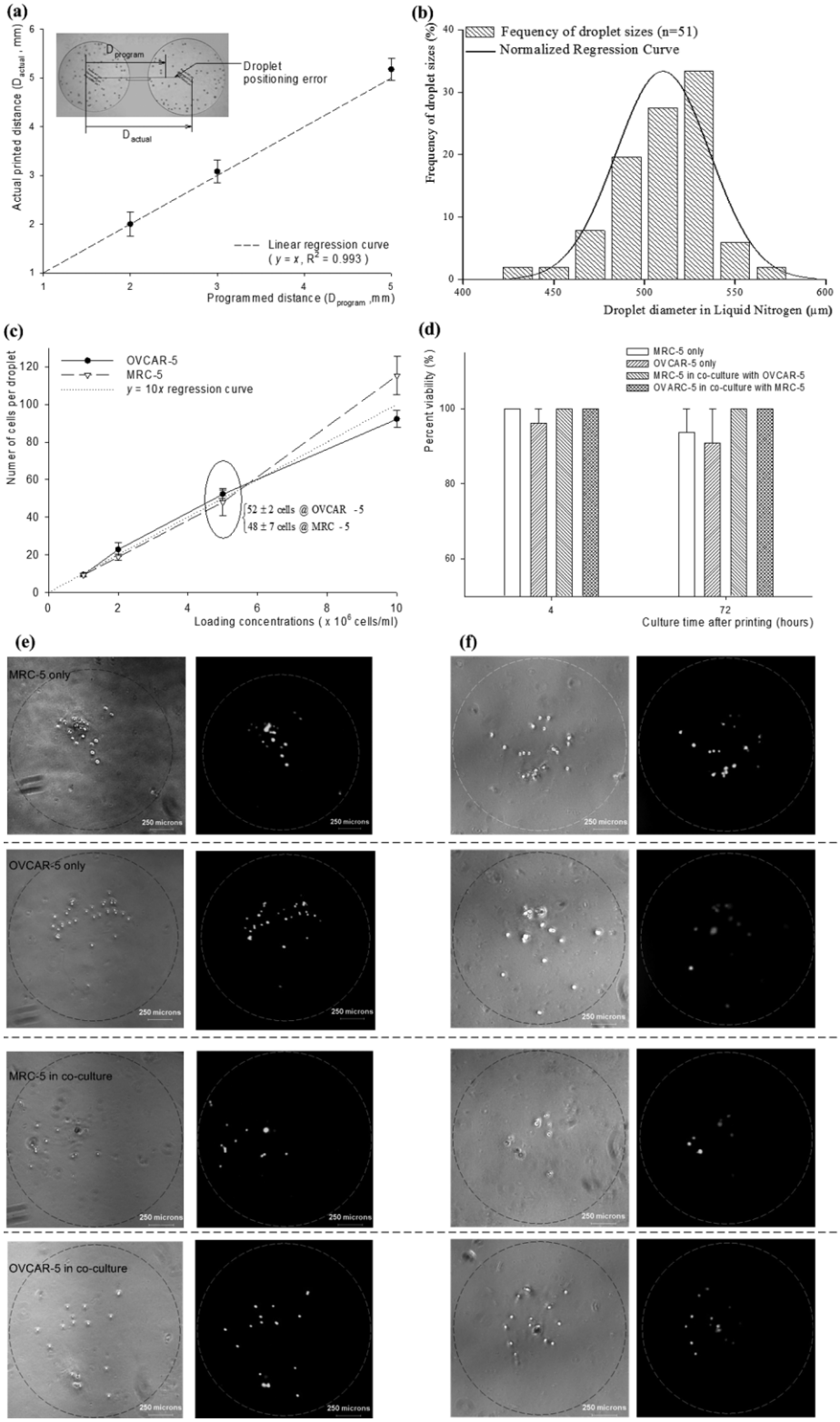

Figure 2. Characterization of the high-throughput cell patterning platform (60 µs valve opening duration and 34.5 kPa nitrogen gas pressure). (a) Droplet positioning accuracy. The positioning error of two droplets is measured by the difference between programmed distance ($D_{program}$) and actual printed distance of droplets after patterning (D_{actual}); R^2=0.9932. (b) Droplet size distribution, measured in liquid nitrogen, was 510 ± 26 µm. Droplet size was obtained from 51 droplets. (c) Number of cells per droplet for OVCAR-5 and MRC-5. (d) Percent viability of OVCAR-5 and MRC-5 coculture after printing (4 h) and at day 3 (72 h) with respect to flask cell viability (n=4). (e. f) Live/dead staining to calculate percent viability at (d). Scale bars, 250 µm.

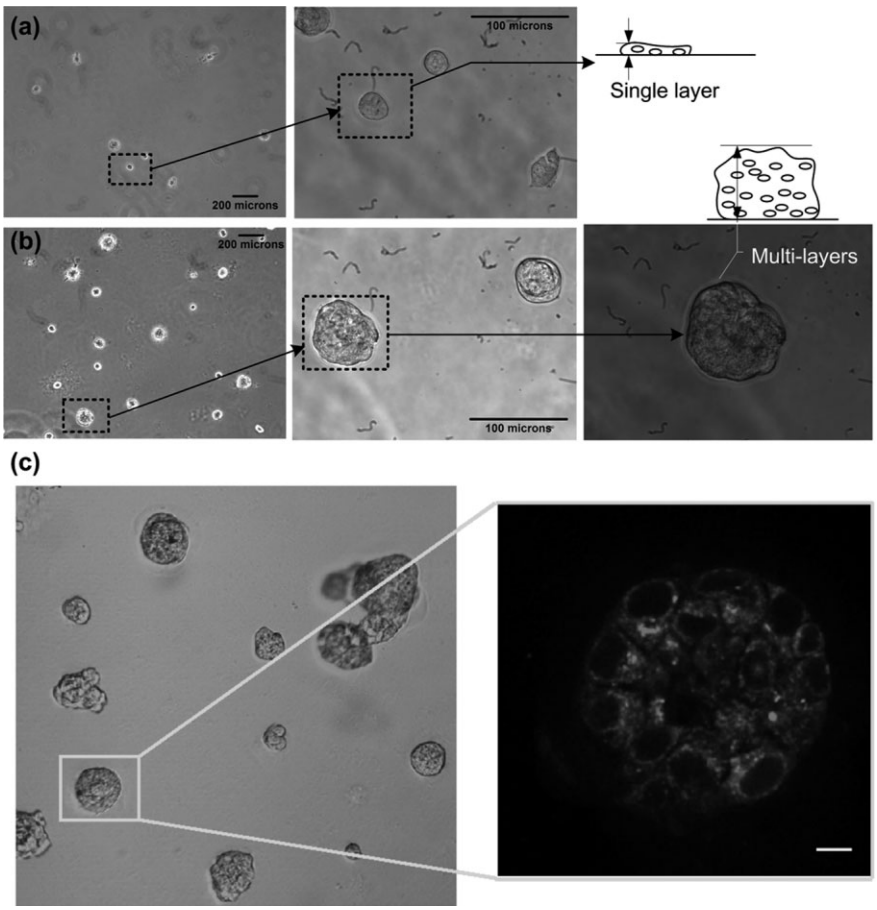

Figure 3. 3D acini formation in GFR Matrigel™. OVCAR5 cells are printed on Matrigel™ substrate and grown in culture medium. Two-photon autofluorescence images show the 3D structure of 3D acini formed from ovarian cancer cells 7 days following printing. Scale bar, 20 μm.

20 000 droplets/min for each cell type. With on average 100 cells per droplet, this platform can pattern 2 million OVCAR-5 cells and fibroblasts per minute.

3.2 Acini formation in a 3D microenvironment

We compared the growth and development of our patterned 3D cultures with previously characterized growth properties of ovarian 3D acini formed from manually pipetted cells [13, 14]. Two-photon images show representative 3D acinar structure 7 days post patterning (Fig. 3). This 3D structure qualitatively recapitulates the micronodular feature of ovarian cancer that was observed in pipetted models [13, 14] and in vivo [2, 29–31].

We also characterized the kinetics of acini growth by tracking the patterned cancer cells for up to 15 days after patterning. The size (calculated as the cross-sectional area from the 2D microscopy image) and number of the 3D acini at multiple time points were quantified (Figs. 4a–c) using a previously described custom-developed MATLAB program [14]. The size distribution of the 3D acini changes significantly with culture time (Fig. 4a and Table 1). We observed that the distribution of acinar sizes started from a small range (~100–500 μm^2 at day 1), but the range consistently broadened with culture time, as indicated by the increased number of acini with larger size (days 5, 9, 15) (Fig. 4a). This may be due to the combined effect of cell proliferation and acini fusion via migration and coalescence [13, 14]. This heterogeneity in acinar size is consistent with that observed in manually pipetted models [13, 14] and in vivo [30, 31]. We also observed a significant fraction in the 200–400 μm^2 size range at all time points, and another fraction that developed more rapidly into larger structures over time. This overall growth pattern is consistent with that previously reported for 3D growth resulting from manually pipetted cells [13, 14]. Figure 4b show the change in number of acini as a function of number of initial cells per droplet. More acini were obtained with higher initial number of cells per droplet. However, the number decreases continuously with culture time and gets to a stable state after day 9 independent of the initial cell concentration. These observations agree with the results pre-

Table 1. 3D acini size distribution according to culture duration from 1 to 15 days

Size (μm)	Day 1	Day 5	Day 7	Day 8	Day 9	Day 15
100	0.0	0.0	0.0	0.0	0.0	0.0
200	22.4	19.6	28.6	19.4	29.4	28.1
300	52.2	17.6	9.5	27.8	23.5	21.9
400	14.9	13.7	9.5	8.3	14.7	15.6
500	1.5	15.7	14.3	2.8	2.9	0.0
600	1.5	2.0	7.1	5.6	5.9	3.1
700	4.5	7.8	4.8	11.1	0.0	3.1
800	1.5	9.8	2.4	0.0	2.9	3.1
900	0.0	0.0	0.0	2.8	0.0	6.3
1000	1.5	2.0	2.4	2.8	0.0	0.0
>1000	0.0	11.8	21.4	19.4	20.6	18.8

viously reported for 3-D acini formed from manually pipetted cells [13, 14]. The average size of ovarian cancer acini increased exponentially with culture time (Fig. 4c). The ability to obtain uniform-sized acini is of great importance for cancer study, e.g., the drug response of different sized acini. Using our current method, multiple acini were formed in individual printed droplet. To decrease the num-

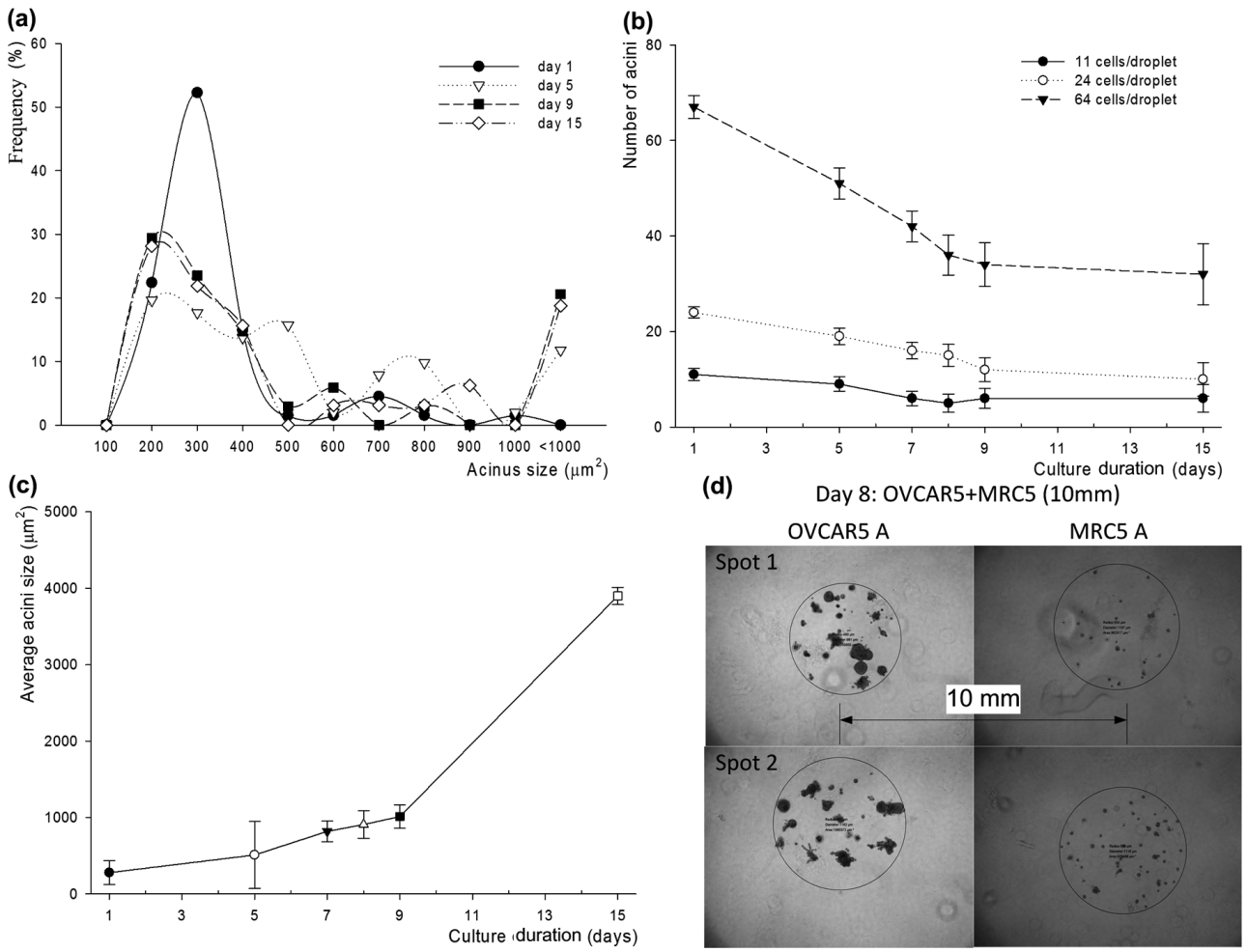

Figure 4. Acini growth kinetics after patterning. (a) 3D acini size distribution according to culture duration from 1 to 15 days. (b) Number of acini changing as a function of initial number of cells per droplet. (c) Average acini size increases with culture time. (d) Bright-field image of OVCAR-5 and MRC-5 cells after 8 days of coculture.

ber of acini per droplet, one approach could be to decrease the droplet size or the cell concentration in the ejection reservoir. Another approach might be to use non-adhesive microwell arrays, which have been utilized to form uniform-sized embryoid bodies (EB) [32–35].

4 Conclusions

In this study, we micropatterned ovarian cancer cells (OVCAR-5) and fibroblasts (MRC-5) with spatial control. We characterized the biopatterned OVCAR-5 and MRC-5 for the number of cells per droplet, droplet size and cell viability. We also investigated printed acini growth kinetics such as change in acini size and number over time. The results show that both OVCAR-5 and MRC-5 can be ejected with controlled number of cells per droplet maintaining high viability. Microprinted OVCAR-5 remained viable and proliferated in Matrigel forming 3D acinar structures. The acinar growth kinetics in the patterned model resemble that of 3D acini formed from cells originally ejected by manual pipetting, and similarly recapitulate features of ovarian cancer micronodules in vivo.

The developed model system with spatial patterning of cell types and the initial cell density control in patterned constructs would enable physiologically relevant ovarian cancer coculture models to be created for a better understanding of ovarian cancer biology and improved clinical therapies. As a future application, such a platform could be used to build in vitro disease models in which various cell types are required to be placed with precise spatial control. This would allow systematic investigation of the many unknown regulatory feedback mechanisms between cells in a well-defined 3D environment, e.g. tumor and stromal cells for cancer. In addition, the model constructs fabricated at high throughput using this platform could be used in high-throughput screening of drug and treatment responses for reliable statistical analysis, reducing the testing costs and supporting alternative physiological models to animal testing.

U.D. would like to thank the Randolph Hearst Foundation and the Department of Medicine, Brigham and Women's Hospital for the Young Investigators in Medicine Award. We thank Jie (Jenny) Zhao, Director of the Photopathology core of the Wellman Center for Photomedicine for her assistance with multiphoton fluorescence imaging. I.R. gratefully acknowledges support from the Wellman Center for Photomedicine in the form of a Wellman Fellowship. We thank Drs. Conor Evans and Adnan Abu-Yousif of the Wellman Center for several useful discussions of this work. This work was performed at both the Bio-Acoustic MEMS in Medicine (BAMM) Laboratories at the Center for Bioengineering, Brigham and Women's Hospital and Harvard Medical School and at the Wellman Center for Photomedicine at the Massachusetts General Hospital and Harvard Medical School. Funding was provided by the National Institutes of Health, 5R01CA119388-03 (to T.H.), P01CA084203-06 (to T.H.) and R21 (EB007707). UD and FX were partially supported by the Center for Integration of Medicine and Innovative Technology (CIMIT) under US Army Medical Research Acquisition Activity Cooperative Agreement – New Development Grant.

The authors have declared no conflict of interest.

5 References

[1] Jemal, A., Siegel, R., Ward, E., Hao, Y. *et al.*, Cancer statistics, 2008. *CA Cancer J. Clin.* 2008, *58*, 71–96.
[2] Cho, K. R., Shih, I. M., Ovarian cancer. *Annu. Rev. Pathol. Mech. Dis.* 2009, *4*, 287–313.
[3] Orimo, A., Gupta, P. B., Sgroi, D. C., Arenzana-Seisdedos, F. *et al.*, Stromal fibroblasts present in invasive human breast carcinomas promote tumor growth and angiogenesis through elevated SDF-1/CXCL12 secretion. *Cell* 2005, *121*, 335–348.
[4] Olumi, A. F., Grossfeld, G. D., Hayward, S. W., Carroll, P. R. *et al.*, Carcinoma-associated fibroblasts direct tumor progression of initiated human prostatic epithelium. *Cancer Res.* 1999, *59*, 5002–5011.
[5] Dong, Z., Nor, J. E., Transcriptional targeting of tumor endothelial cells for gene therapy. *Adv. Drug Deliv. Rev.* 2009, *61*, 542–553.
[6] Dudley, A. C., Klagsbrun, M., Tumor endothelial cells have features of adult stem cells. *Cell cycle* 2009, *8*, 236–238.
[7] Sappino, A. P., Skalli, O., Jackson, B., Schurch, W., Gabbiani, G., Smooth-muscle differentiation in stromal cells of malignant and nonmalignant breast tissues. *Int. J. Cancer* 1988, *41*, 707–712.
[8] Kenny, H. A., Krausz, T., Yamada, S. D., Lengyel, E., Use of a novel 3D culture model to elucidate the role of mesothelial cells, fibroblasts and extra-cellular matrices on adhesion and invasion of ovarian cancer cells to the omentum. *Int. J. Cancer* 2007, *121*, 1463–1472.
[9] Kalluri, R., Zeisberg, M., Fibroblasts in cancer. *Nat. Rev. Cancer* 2006, *6*, 392–401.
[10] Cho, C. H., Park, J., Tilles, A. W., Berthiaume, F. *et al.*, Layered patterning of hepatocytes in co-culture systems using microfabricated stencils. *Biotechniques* 2010, *48*, 47–52.
[11] Hui, E. E., Bhatia, S. N., Micromechanical control of cell-cell interactions. *Proc. Natl. Acad. Sci. USA* 2007, *104*, 5722–5726.
[12] Park, T. H., Shuler, M. L., Integration of cell culture and microfabrication technology. *Biotechnol. Prog.* 2003, *19*, 243–253.
[13] Rizvi, I., Celli, J. P., Evans, C. L., Abu-Yousif, A. O. *et al.*, Synergistic enhancement of carboplatin efficacy with photodynamic therapy in a three-dimensional model for mi-

crometastatic ovarian cancer. *Cancer Res.* 2010, *70*, 9319–9328.

[14] Celli, J. P., Rizvi, I., Evans, C. L., Abu-Yousif, A. O., Hasan, T., Quantitative imaging reveals heterogeneous growth dynamics and treatment-dependent residual tumor distributions in a three-dimensional ovarian cancer model. *J. Biomed. Opt.* 2010, *15*, 051603–051610.

[15] Demirci, U., Montesano, G., Single cell epitaxy by acoustic picolitre droplets. *Lab Chip* 2007, *7*, 1139–1145.

[16] Demirci, U., Acoustic picoliter droplets for emerging applications in semiconductor industry and biotechnology. *J. Microelectromech.Syst.* 2006, *15*, 957–966.

[17] Demirci, U., Montesano, G., Cell encapsulating droplet vitrification. *Lab Chip* 2007, *7*, 1428–1433.

[18] Boland, T., Xu, T., Damon, B., Cui, X., Application of inkjet printing to tissue engineering. *Biotechnol. J.* 2006, *1*, 910–917.

[19] Chang, R., Nam, J., Sun, W., Direct cell writing of 3D microorgan for in vitro pharmacokinetic model. *Tissue Eng.* 2008, *14*, 157–166.

[20] Mironov, V., Visconti, R. P., Kasyanov, V., Forgacs, G. *et al.*, Organ printing: Tissue spheroids as building blocks. *Biomaterials* 2009, *30*, 2164–2174.

[21] Roth, E. A., Xu, T., Das, M., Gregory, C. *et al.*, Inkjet printing for high-throughput cell patterning. *Biomaterials* 2004, *25*, 3707–3715.

[22] Puttaswamy, S. V., Sivashankar, S., Chen, R.-J., Chin, C.-K. *et al.*, Enhanced cell viability and cell adhesion using low conductivity medium for negative dielectrophoretic cell patterning. *Biotechnol. J.* 2010, *5*, 1005–1015.

[23] Young, E. W., Beebe, D. J., Fundamentals of microfluidic cell culture in controlled microenvironments. *Chem. Soc. Rev.* 2010, *39*, 1036–1048.

[24] Park, J. W., Kim, H. J., Byun, J. H., Ryu, H. R., Jeon, N. L., Novel microfluidic platform for culturing neurons: culturing and biochemical analysis of neuronal components. *Biotechnol. J.* 2009, *4*, 1573–1577.

[25] Xu, F., Moon, S., Emre, A. E., Turali, E. S. *et al.*, A droplet based building block approach for bladder smooth muscle cell (SMC) proliferation. *Biofabrication* 2010, *2*, 014105.

[26] Moon, S., Hasan, S. K., Song, Y. S., Xu, F. *et al.*, Layer by layer three-dimensional tissue epitaxy by cell-laden hydrogel droplets. *Tissue Eng. Part C Methods* 2010, *16*, 157–166.

[27] Song, Y. S., Adler, D., Xu, F., Kayaalp, E. *et al.*, Vitrification and levitation of a liquid droplet on liquid nitrogen. *Proc. Natl. Acad. Sci. USA* 2010, *107*, 4596–4600.

[28] Rahmanzadeh, R., Rai, P., Celli, J. P., Rizvi, I. *et al.*, Ki-67 as a molecular target for therapy in an in vitro three-dimensional model for ovarian cancer. *Cancer Res.* 2010, *70*, 9234–9242.

[29] Tsai, H. W., Yuan, C. C., Wang, P. H., Umbilicus as the only site of metastasis in recurrent ovarian cancer. *J. Chin. Med. Assoc.* 2006, *69*, 233–235.

[30] Zhong, W., Celli, J. P., Rizvi, I., Mai, Z. *et al.*, In vivo high-resolution fluorescence microendoscopy for ovarian cancer detection and treatment monitoring. *Br. J. Cancer* 2009, *101*, 2015–2022.

[31] Molpus, K. L., Koelliker, D., Atkins, L., Kato, D. T. *et al.*, Characterization of a xenograft model of human ovarian carcinoma which produces intraperitoneal carcinomatosis and metastases in mice. *Int. J. Cancer* 1996, *68*, 588–595.

[32] Karp, J. M., Yeh, J., Eng, G., Fukuda, J. *et al.*, Controlling size, shape and homogeneity of embryoid bodies using poly(ethylene glycol) microwells. *Lab Chip* 2007, *7*, 786–794.

[33] Hwang, Y. S., Chung, B. G., Ortmann, D., Hattori, N. *et al.*, Microwell-mediated control of embryoid body size regulates embryonic stem cell fate via differential expression of WNT5a and WNT11. *Proc. Natl. Acad. Sci. USA* 2009, *106*, 16978–16983.

[34] Lee, W. G., Ortmann, D., Hancock, M. J., Bae, H., Khademhosseini, A., A hollow sphere soft lithography approach for long-term hanging drop methods. *Tissue Eng.* 2010, *16*, 249–259.

[35] Choi, Y. Y., Chung, B. G., Lee, D. H., Khademhosseini, A. *et al.*, Controlled-size embryoid body formation in concave microwell arrays. *Biomaterials* 2010, *31*, 4296–4303.